Supplementary Figure 1. Imaging setup.

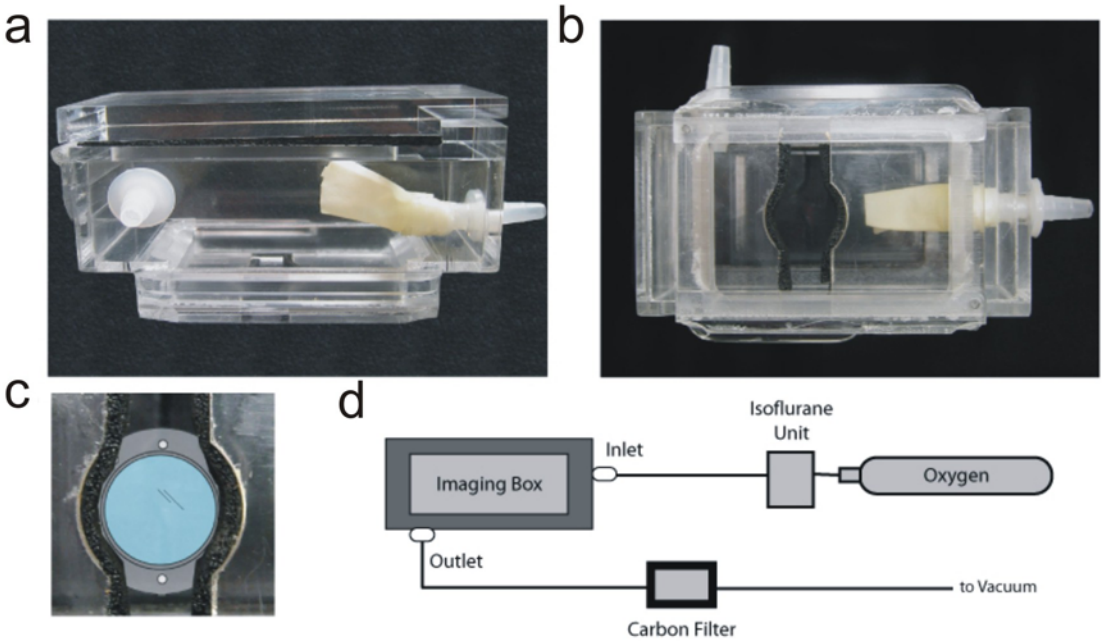

View from the side (**a**) or the bottom (**b**) of the imaging box that was used to anesthetize and to immobilize the mouse for imaging. (**c**) For imaging Z-stacks, the imaging window was securely immobilized between two doors in the bottom of the box. (**d**) A flow of isoflurane enters the imaging box through a nozzle, and due to the negative pressure, the isoflurane exits the box passing through a carbon filter.

Supplementary Figure 2. Comparative histology of Dendra2-MTLn3 tumors with and without MIW implant.

a

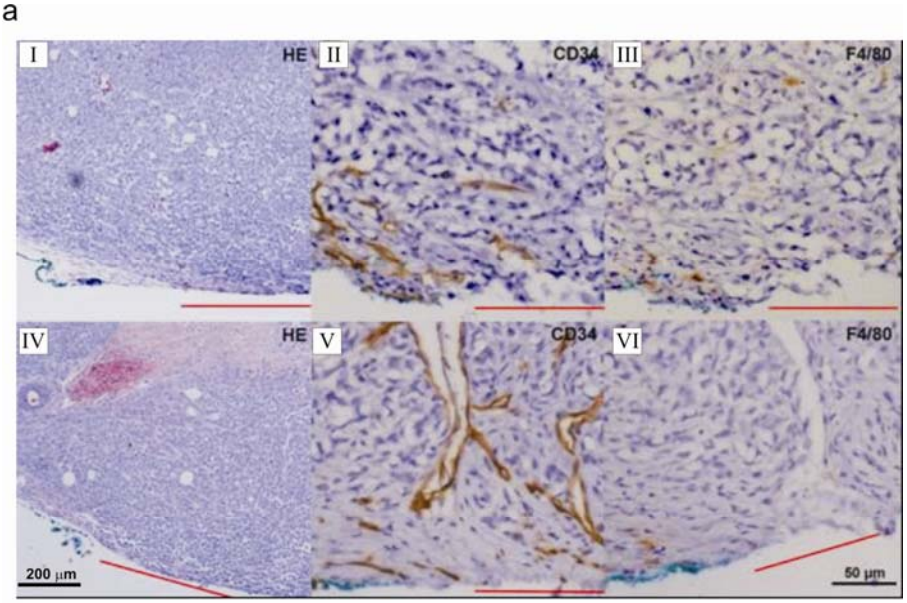

b

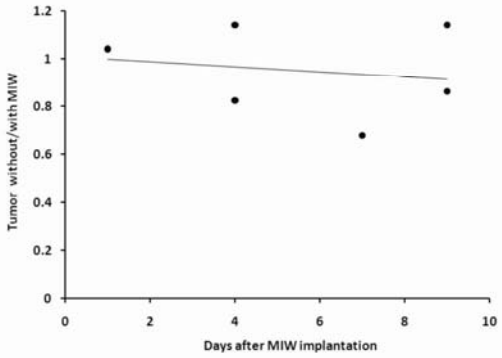

c

Dendra2	MIW	Photoswitch	$N_{vessels}/mm^2$	$N_{macrophages}/mm^2$	$d_{edge\text{-}necrotic\ zone}$ (mm)
-	-	-	91 +/- 3.0	10 +/- 5.4	0.4 +/- 0.24
+	-	-	53 +/- 13.7	8 +/- 3.0	1.3 +/- 0.92
+	+	-	44 +/- 4.2	10 +/- 3.8	0.5 +/- 0.45
+	+	+	48 +/- 10.7	8 +/- 3.2	0.8 +/-0.54

(**a**) (I- III) control tumors without window, (IV- VI) tumors with MIW implant; (I, IV) H&E sections, scale bar 200 µm; (II, V) blood vessel staining using CD34 antibody (III, VI) macrophages stained using F4/80, scale bar 50 µm. Tumors were dissected from the connective tissue and the mammary fat; the surfaces away from the MIW (or away from the skin) were marked with green tissue dye for orientation. In the sections shown, red dashed lines mark tumor areas where MIW was located (IV-VI) or corresponding areas next to the skin in control tumors

(I-III). Tumors were formalin-fixed and stained using H&E to visualize necrotic areas, general morphology, mitosis and apoptotic cells; CD34 antibody to visualize angiogenesis and F4/80 antibody to visualize possible inflammation. (**b**) Change in tumor volume due to MIW insertion.At day 0, before the MIW insertion, tumor size was measured through the skin and animals with equal tumor sizes were marked as control-MIW pairs, with one member of each pair receiving a MIW and the other member of the pair left as the control. At 1, 4, 7 or 9 days after the MIW insertion, both members of the control-MIW pair were euthanized, the tumors removed and dimensions were measured. The ratio without MIW to with MIW was calculated for tumor volume. Regression analysis indicates no significant change in relative tumor volume with time (slope =-0.011, S.E. of slope = 0.029, $p < 0.73$) and no significant change in relative tumor volume of tumors analyzed at day 4, 7 or 9 compared to 1. (**c**) Quantitation of histological sections. Tumors with and without the Dendra2 transgene, MIW and photoswitching 24 h prior to fixation are compared in number of vessels (based on CD34 staining) and macrophages (based on F4/80 staining) and distance from the tumor edge to the closest necrotic zone. All the measurements were done in the areas covered by MIW or skin (in the control tumors without MIW). T-tests showed no statistical significance between populations.

Supplementary Figure 3. Quantification of invasion and intravasation of adenocarcinoma cells in different tumor microenvironments.

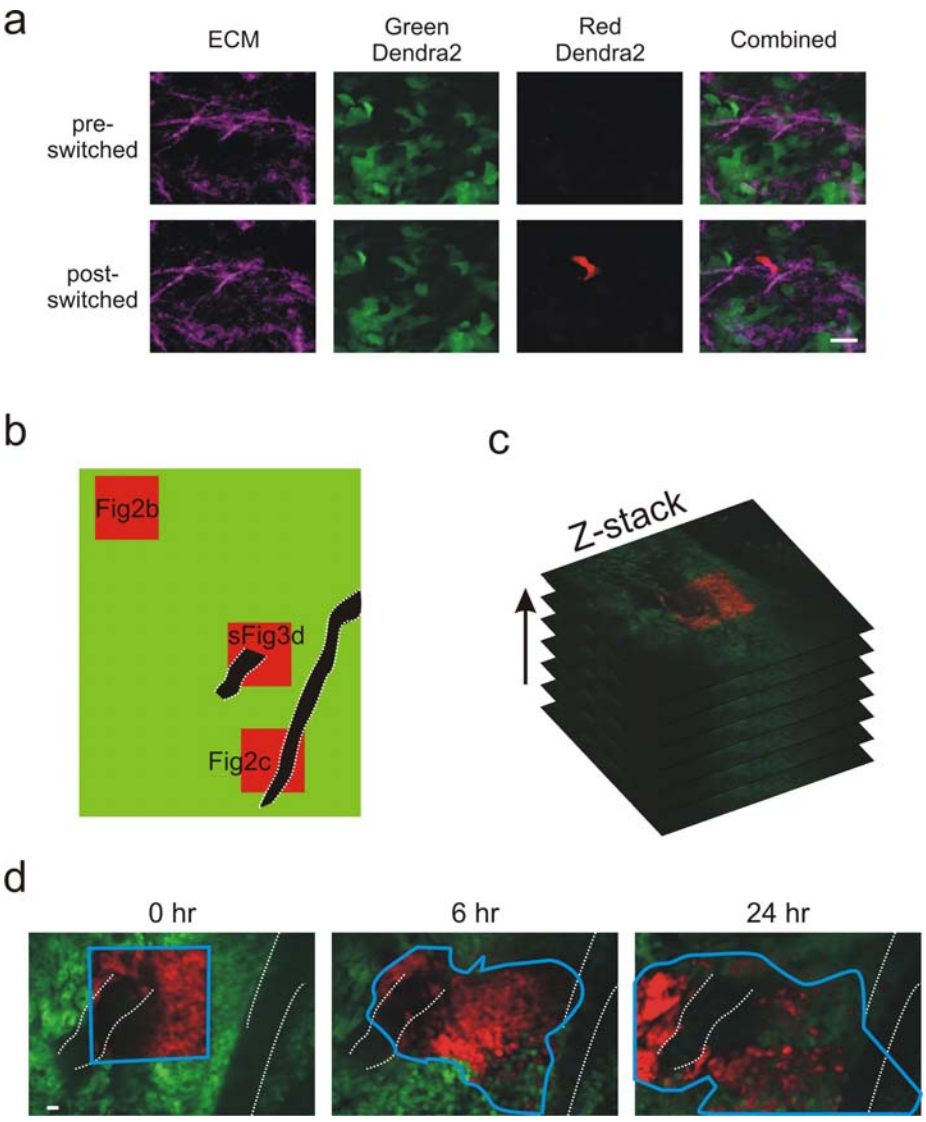

(**a**) Visualization of multiple channels during intravital photo-switching of a single Dendra2-MTLn3 cell. Green and red channels represent Dendra2 before and after photo-switching while purple denotes extracellular matrix visualized (ECM) via light scattering. (**b**) Diagram of three regions (250 x 250 μm) within the same orthotopic tumor that were photoswitched. Dark areas represent visible blood vessels, while the red areas represent the sites of photoswitching. sFig3d = Supplementary Fig. 3d. (**c**) Z-stacks of these regions were acquired at 0, 6 and 24 hours after photoswitching. (**d**) Single z-sections are shown. Maximum projections of the full z-stacks were made and the infiltration area (the area in which cells can be found as shown with the blue line) and numbers of photoswitched cells were measured over time.

Supplementary Figure 4. Genetically encoded and transiently transfected tumor models can be visualized through the MIW.

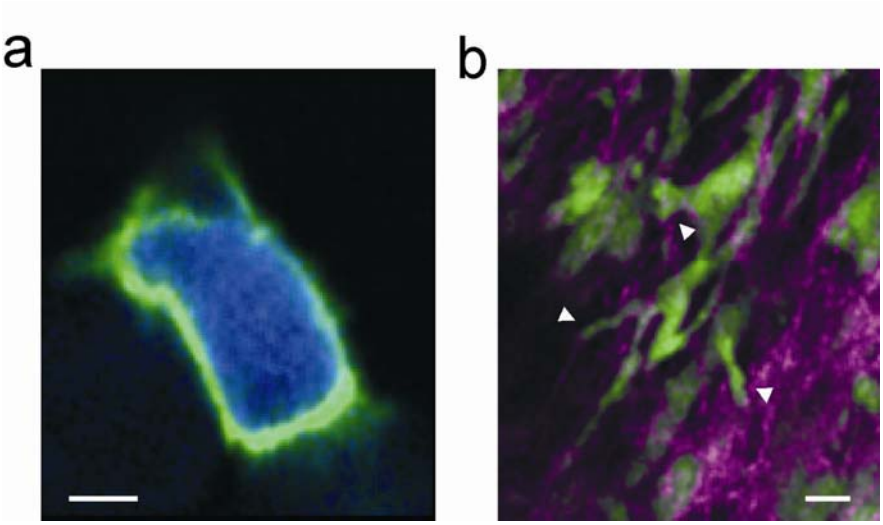

(**a**) MTLn3 cells that stably express cytosolic CFP were transiently transfected with a membrane targeted GFP (GFP-CAAX), and injected into the mammary fat pad. Several days after inoculation, high resolution CFP (blue) and GFP (green) images were acquired through the MIW (scale bar 5 μm). **(b)** The MIW was inserted on top of a MMTV-PyMT GFP+ tumor. Images were acquired of tumor cells (green) and the ECM (purple). Notice the interactions (arrowheads) between the cells and the matrix fibers (scale bar 10 μm).

Supplementary Methods:

Cell Culture

MTLn3 cells, originally isolated by Neri and Nicolson (Institute for Molecular Medicine, Huntington Beach, CA), were maintained in αMEM (Life Technologies, Inc., Gaithersburg, MD) with 5% FBS and penicillin-streptomycin (Life Technologies, Inc.). *Dendra2* was in the cloning vector C1 with the G418 selection marker. Transfection was done using Lipofectamine 2000 (Invitrogen, CA). Sorting of the cells was done using FACS 72 h after the transfection; 4% of the cells expressing the highest fluorescence levels were kept for culturing and selection was maintained using 500 μg/ml G418 geneticin (Invitrogen, CA). We have not observed any changes in cell morphology, viability or proliferation in Dendra2-MTLn3 cells compared to GFP-MTLn3 cells.

Choice of the photoswitchable protein

Photoswitchable fluorescent proteins represent a group of fluorescent proteins which all exhibit high level of amino acid identity with EGFP; they are genetically encoded probes which allow instant labeling of proteins, organelles or cells with light of a specific wavelength. In contrast to so called photoactivatable proteins, such as photoactivatable GFP, which do not fluoresce before photoconversion (i.e., are dark), the photoswitchable proteins are already fluorescent in one spectral range and then change the fluorescence spectrum after a brief light irradiation. Currently, there are two types of the protein that are photoswitching either from cyan to green or from green to red. Since cellular and tissue autofluorescence tends to decrease with increasing wavelength, we prefer to use the latter type. Also, among the green-to-red phototoswitchable proteins there are monomeric as well as tetrameric proteins. Tetrameric fluorescent proteins such as DsRed are known to frequently cause formation of intracellular aggregates and a significant decrease in viability which complicates establishing of stable clones. This is why we decided to use the monomeric green-to-red protein, Dendra2. Additional advantages of Dendra2 over the other monomeric green-to-red proteins are that it completely forms a functional chromophore at 37 $^{\circ}$C, which is not the case for mEosFP, and it is substantially brighter than the original Dendra protein.

Design of the imaging window

Mammary Imaging Window (MIW) base is made from tissue culture-grade plastic dishes (Becton Dickinson #353004) by cutting out ring-shaped pieces. Dimensions of the smaller ring are 9 mm for internal and 10 mm for external diameter, 9 mm/14 mm for larger ring. This design assures MIW touches the mammary gland surface while allowing for suturing and proper window positioning inside the imaging box. Both parts are sanded and glued together. In order to secure the window in the animal, 8 suturing holes are made on the larger piece. Holes were equally positioned around the edge of the smaller ring. The coverslip (8 mm, #1, circular, custom made by Fisher Scientific) was attached to the top of the small ring using superglue. Further, MIW was rinsed with sterile water and ethanol, dried and placed under the UV light in the tissue culture dish for at least 12 h on each side.

Window insertion surgery

Female 5- to 6-week-old BALB/c SCID/Ncr mice were purchased from the National Cancer

Institute and housed in a pathogen-free barrier facility until use. Mice were first injected with 10^6 MTLn3 cells in the abdominal mammary fat pad. After 15-17 days, when the tumor reached 0.5 cm in diameter, the window was inserted under the skin on top of the tumor. Surgeries were done in the quarantine room according to the survival surgery protocol approved by AECOM Animal Institute. A sterile cloth is placed inside a laminar flow hood, with a heating pad (36 ºC) under it. Sterile dissecting scissors, tweezers, cotton swabs and suturing thread were placed on the cloth. Mice were anesthetized with intraperitoneal injection of 0.35 ml of Tribromo-ethanol (Avertin 2 %) and placed on a piece of gauze. The tumor surface was shaved and the rest of the hair was removed with lotion hair remover. The skin was disinfected with 70 % EtOH and Betadine, and the mouse was transferred on the sterile cloth. The skin dissection was started at the nipple area and no skin was cut away. A 5mm long incision was made and the skin above the tumor was dissected away from the tumor using micro-dissecting scissors 3-1/4" (BRI, Inc. #11-1080). Once enough of the surface of the tumor was detached from the skin, a sterile window was inserted under the skin and positioned so the glass touches the intact tumor. The skin was placed over the MIW edge and sutured through the holes to secure the MIW in place. Tissue glue (cyanoacrylate tissue adhesive) was used to seal the suturing holes and attach the window to the edges of the skin. The animal was allowed to recover and placed back into the cage. As a prophylaxis, TMP-SMX antibiotic (Hi-Tech Pharmacal #NDC 50383-824-16) is given by supplementing the water bottle with 3 ml of the antibiotic solution. Imaging was done 2-9 days after surgery.

Image Acquisition and Analysis

Isoflurane (Aerrane) was used to sedate the mice during short imaging sessions. The anesthetized animal was placed inside a custom box designed to maintain a temperature of 32 C°. The box introduces isoflurane through a face mask and exchanges air through an inlet and outlet. The MIW was secured at the bottom of the box, with the coverslip exposed through an opening facing the objective of the microscope. A Leica TCS SP2 AOBS confocal microscope (Mannheim, Germany) was used for intravital imaging. The microscope is equipped with 63x (Leica HCX PL APO, NA 1.3, WD 0.6 mm) and 20x (HC PL APO NA 0.7, WD 1 mm) glycerol objectives. Similar results can be obtained with a multiphoton microscope with greater maximal depth of imaging. The argon laser 488 nm line was used at up to 10 % for imaging of the green Dendra2 variant and ECM (averaging 60 µW through the objective). Photoswitching was done using full power of a blue diode laser emitting at 405 nm (average power 10 µW through the objective) with 4.9 µs dwell time per pixel. Excitation of the red Dendra2 variant was done using up to 15 % power of a red diode laser emitting at 561 nm (averaging 30µW at the objective), and excitation of AlexaFluor647-10K dextran using up to 20 % HeNe laser power at 633 nm. Green Dendra2 variant fluorescence was collected between 510-560 nm; red Dendra2 fluorescence was collected between 580-620 nm, AlexaFluor647-10K dextran fluorescence was collected between 650-700 nm, and the ECM scattering was collected between 470-500 nm. Z-stacks were obtained up to a depth of 40-60 µm into the tissue. Multiphoton microscopy allowed for imaging ~100 µm deep into the tissue. Multiphoton images of photoswitched Dendra were acquired with a BioRad Radiance 2000 Multiphoton Microscope using an inverted Olympus IX70 microscope and a 40x 0.9 NA. The two-photon microscope is equipped with 450/30 emission filter for second harmonic light, 536/40 for collection of Dendra2 emission pre-photoswitching and 593/40 for Dendra2 post-switching. Z-stack presented in Supplementary movie 3 was obtained using 860 nm excitation light delivered by Tsunami laser averaging 200 mW at the objective. The collected

512x512 pixels Z-stacks were stored and analyzed with Image J (Rasband, W.S., ImageJ, U. S. National Institutes of Health, Bethesda, MD, USA, http://rsb.info.nih.gov/ij/, 1997-2006). For migration analysis, a maximum projection was generated for the red photoswitched Z-stack, and the area in which photoswitched cells were found was measured, and normalized to the area at time 0. RGB images were processed as an OR function between Red and Green channels. The number of cells was counted in the z-stack, and multiple counts of the same cell in different slices were avoided by marking cells in each plane with a custom ImageJ plug-in. In dense areas, a size threshold was applied: each peak in fluorescence of maximum width <10 μm around the center was defined as a single cell. Results represented for Dendra2 MTLn3 cells were similar to those of Eos (tetrameric photoswitchable protein) in MTLn3 cells (total *in vivo* experiment N>20).

Equipment and settings for every figure

Figure 1: Images (512 x 512 pixels, 8 bits) of a MTLn3-dendra tumor were acquired through the MIW using a Leica TCS SP2 AOBS confocal microscope (Mannheim, Germany) equipped with a 20x (HC PL APO NA 0.7, WD 1 mm) glycerol objectives at 32 C°. Photoconversion was done with a 405 nm laser. For excitation of the green Dendra 2, the argon laser 488 nm line was used, and for the red Dendra 2 a red diode laser emitting at 561 nm. Green Dendra2 variant fluorescence was collected between 510-560 nm; red Dendra2 fluorescence was collected between 580-620 nm. In Fig. 1e, the acquired images were processed with Image J using an OR function between Red and Green channel that works as follow: Only the pixels in the red channel that are above background are shown, and for all other pixels, the green channel is shown.

Figure 2: XYZ stacks (512 x 512 pixels, 8 bits) of a MTLn3-dendra tumor were acquired through the MIW using a Leica TCS SP2 AOBS confocal microscope (Mannheim, Germany) equipped with a 20x (HC PL APO NA 0.7, WD 1 mm) glycerol objectives at 32 C°. Photoconversion was done with a 405 nm laser. For excitation of the green Dendra 2, the argon laser 488 nm line was used, and for the red Dendra 2 a red diode laser emitting at 561 nm. Green Dendra2 variant fluorescence was collected between 510-560 nm; red Dendra2 fluorescence was collected between 580-620 nm. AlexaFluor647-10K dextran fluorescence upon 633 nm excitation was collected between 650-700 nm, and the ECM scattering upon 488 nm excitation was collected between 470-500 nm. All RGB images were generated in Image J. In Fig. 2a-c, the acquired images were processed with Image J. Three images of the Z-stack were averaged and a RGB image was generated using an OR function between Red and Green channel that works as follow: Only the pixels in the red channel that are above background are shown, and for all other pixels, the green channel is shown. For calculating the infiltration area, a maximum projection of the Z-stacks were generated in Image J, and the area in which photoswitched cells were found was measured, and normalized to the area at time 0.

Detection of photoswitched cells in the lung

Lungs of an animal which had a large area (20 mm^2) of the primary tumor photoswitched were examined *ex vivo* 24h after photoswitching in green and red channels by epifluorescence microscopy. In the green channel, only single green cells were taken into account. The average number of single green cells was 1.4 +/- 0.33 cells / mm^2 and average number of red cells was 0.009 +/- 0.007 cells / mm^2, resulting in green/red ratio of 152.

This number of cells is close to what can be expected theoretically: The photoswitched volume is 2 mm^3 when photoswitched cells are positioned inside the window surface area (20

mm^2) and a 0-0.1 mm depth of switching is assumed. Knowing that average tumor volume is 523 mm^3 (average size measured at 4 days post-implantation of the MIW , data not shown)) the number of the tumor cells that can be photoswitched is 0.38 % of total cells, only some of which will be adjacent to blood vessels. This means the ratio of green/red cells in the lungs should equal 0.9962 / 0.0038 = 262 in case all the red cells were in areas close to vessels, and larger if some of them were far from the vessels.